

PHYSICAL REVIEW LETTERS

VOLUME 63

3 JULY 1989

NUMBER 1

Chaos beyond Onset: A Comparison of Theory and Experiment

Gemunu H. Gunaratne,⁽¹⁾ Paul S. Linsay,⁽²⁾ and Michael J. Vinson⁽¹⁾

⁽¹⁾*The James Franck Institute, The University of Chicago, 5640 South Ellis Avenue, Chicago, Illinois 60637*

⁽²⁾*Department of Physics, Massachusetts Institute of Technology, Cambridge, Massachusetts 02139*

(Received 10 April 1989)

The chaotic dynamics from a nonlinear electronic circuit is shown to exhibit the universal topological structure of maps on an annulus. This suggests that the corresponding universality class is large enough to include physical systems. We suggest that low-dimensional strange attractors fall into a few classes, each characterized by distinct universal topological features.

PACS numbers: 05.45.+b

Several routes to chaos in dynamical systems have been proposed and analyzed in detail, the best known being the period doubling¹ and the quasiperiodic routes.² At the onset of chaos, such dynamical systems exhibit scaling, and certain qualitative and quantitative features of the transition are universal.³⁻⁵ Many experimental systems are believed to make similar transitions to chaos, with the path determined by evaluating universal features of the transition that are unique to that path.^{6,7} Some examples of universal quantities that can be used for this purpose are the generalized dimensions⁴ or singularity spectra⁵ of the attracting set and the trajectory scaling function³ of the orbit at the onset.

Much less is known about dynamical systems beyond the onset of chaos. Chaotic experimental systems relax to regions of phase space with very complex structure and zero measure. Generally such objects are fractal, and have structure on ever smaller length scales. They are called strange attractors, and are characterized by metric invariants (which do not change under smooth transformations) such as fractal dimension and Lyapunov exponent. However, they are not universal, and hence do not yield much detailed information about the experimental system: e.g., how to model the dynamics.

An alternative class of invariants that can be used to characterize a strange attractor is the set of all periodic orbits.⁸⁻¹⁰ Periodic orbits are topological invariants; i.e., any change of coordinates will not change the periodicity of an orbit. Thus changing the point of observation or the variable that is being observed in an experiment will not change the cycle structure. This is important since

the characterization of the attractor should be robust.

The significance of the cycles is seen from the following observations. First, since the strange attractor is the set of points of the phase space visited by the orbit after the transients have settled down, motion on it is ergodic. Thus the orbit of any point P on the strange attractor will make arbitrarily close returns to P . Because of the smoothness and nonlinearity of the dynamics, one should in general be able to move P by a small amount so that the close return becomes exact: i.e., there is a periodic point arbitrarily close to P . This means that the periodic points are dense on the strange attractor. Since the motion on the attractor is chaotic, these cycles have to be unstable.

The second important observation is that the structure of the strange attractor in the neighborhood of a periodic point and the motion of points in this neighborhood are determined by the tangent space of the periodic point.⁸ In particular, the eigenvalues give the local scaling observed in strange attractors. The nonlinear attractor can thus be considered as a collection of linear neighborhoods about the periodic points. Since this is a description of all invariant local features of the attractor, it is more desirable than a knowledge of averaged quantities such as the fractal dimension or the Lyapunov exponent. Further, the eigenvalues can be used to evaluate such averaged variables of a strange attractor.^{8,10} It has been suggested that the set of periodic points and their eigenvalues are an optimal measurement of the invariant properties of a strange attractor.⁹ Moreover, the structure of the attractor can be described hierarchically by

the cycles. Thus the gross features of the strange attractor can be captured through the short cycles while the longer cycles are needed to describe the fine-scale features.^{8,9}

Recently it was shown¹¹ that the periodic orbits of a class of strange attractors are universal. It is thus possible to determine if a chaotic experimental system belongs to this class by analyzing the cycles. The present Letter is a report of such a study. The experimental system is a nonlinear electronic circuit to be described below. From its properties at and below criticality, and the structure of the chaotic attractor, we conjecture that maps on an annulus should describe certain topological features of the signal. We then use the universalities described in Ref. 11 to confirm our conjecture.

The nonlinear circuit used in the experiment is shown schematically in Fig. 1. The circuit is driven at a frequency Ω_v and observed at a frequency Ω_o . The drive signal is a sine wave from a Hewlett-Packard HP3325A frequency synthesizer. The entire experiment is under computer control and the data can be analyzed on-line to distinguish between periodic, chaotic, and quasiperiodic response.

If the effect of the diodes and inductances could be neglected we would be observing a harmonic oscillation of frequency Ω_v at a frequency Ω_o . Then the return map would have the form

$$x_{n+1} = x_n + \Omega \pmod{1}, \tag{1}$$

where $\Omega = \Omega_v/\Omega_o$, and x_n is the amplitude of the signal at the n th time step. The effect of the full circuit can be modeled by the addition of a nonlinear term giving

$$x_{n+1} = x_n + \Omega - kF(x_n) \pmod{1}, \tag{2}$$

where $F(x)$ is a nonlinear function, and k is the intensity of the nonlinearity. $F(x)$ is chosen so that the right-hand side of Eq. (2) is monotonic increasing for $k < 1$ and will develop an inflection point when $k = 1$. Maps of this form are a subclass of circle maps² that will exhibit all the properties we study here.¹¹ Equation (2) is not a detailed model of the nonlinear circuit, but only captures a few essential features of its evolution (its "circular" behavior). The theory of Ref. 11 gives topological conse-

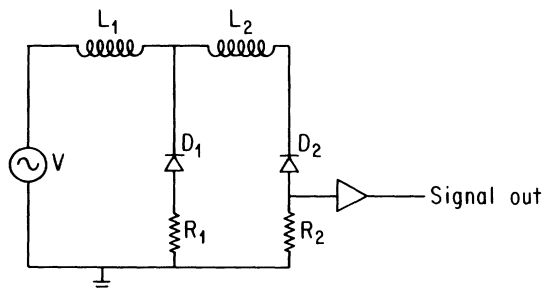


FIG. 1. Schematic representation of the experimental electronic circuit.

quences of such features.

Orbits of Eq. (1) fall into two classes.² If Ω is rational they are periodic, while if it is irrational any orbit will cover the interval ergodically. The average increment of x per iterate (called the winding number) is Ω . When $0 < k < 1$ orbits of Eq. (2), for values of Ω close to rationals ($|\Omega - p/q| \ll 1/q^2$), mode lock to a cycle of rational winding number (p/q). Increasing k generally leads to wider mode-locked regions, leaving ever smaller regions of parameters where the motion is ergodic. The set of parameters for which the map has a given rational winding number is called an Arnold tongue.¹² The form of Arnold tongues for maps of type (2) is shown in Fig. 2. For $k \leq 1$ the monotonicity of Eq. (2) implies that the order of points is preserved under iteration, and that the winding number of an orbit is independent of the starting point.¹² Hence nearby points cannot move arbitrarily far apart, and the motion is nonchaotic.

The parameter space of the electronic circuit is mapped by calculating the winding number for many different sets of control parameters. The structure of Arnold tongues can be seen clearly, and is qualitatively similar to Fig. 2.¹³ Criticality of irrational orbits can be deduced either from the crossing of nearby rational tongues or by studying the Fourier spectrum of the signal.⁶ Critical orbits whose rotation number is $\sigma = (\sqrt{5} - 1)/2$ have been studied in detail,² and invariants of the onset of chaos (e.g., generalized dimensions⁶ and scaling functions⁷) have been shown to be identical to maps of form (2).

For $k > 1$ the winding number of an orbit of Eq. (2) depends on the starting point, and hence nearby points can diverge from each other, giving chaotic motion. The signal from the electronic circuit shows the same behavior. However, the experimental attractor is no longer one dimensional, but contains foldbacks as seen in Fig. 3. Since one-dimensional models cannot support such attractors, Eq. (2) has to be generalized to higher dimensions, for example, as

$$\begin{aligned} r_{n+1} &= br_n - kF(\theta_n), \\ \theta_{n+1} &= \theta_n + \Omega + r_{n+1} \pmod{1}, \end{aligned} \tag{3}$$

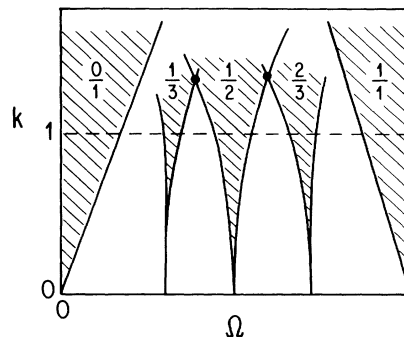


FIG. 2. The structure of the Arnold tongues for Eq. (2).

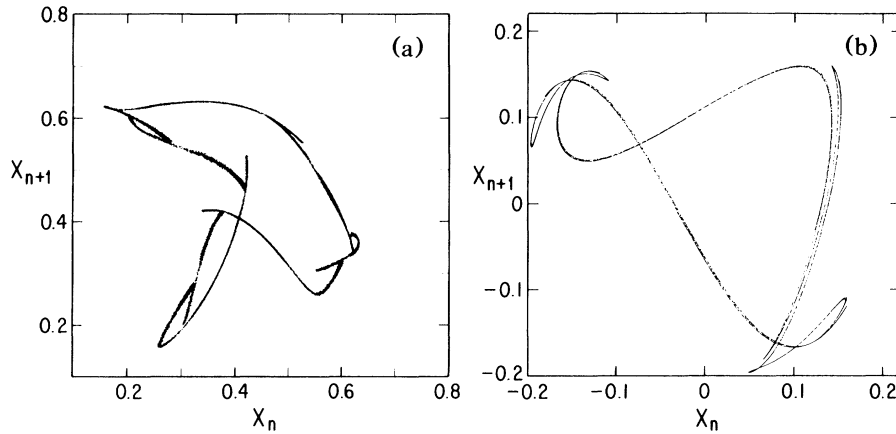


FIG. 3. (a) An experimental attractor. (b) A strange attractor for Eq. (3). Its structure is similar to that of the experimental attractor.

where b is the Jacobian of the map, and its inverse measures the effective dissipation. Maps of this form have chaotic attracting sets like that of Fig. 3.¹² Reference 11 shows that unstable periodic orbits on chaotic attractors of such maps have universal features, and we look for them in the experimental signal.

Certain points in the parameter space of Eq. (2) can be defined topologically. For example, there are a countable set of points that are the crossings of two Arnold tongues (other possibilities include the crossing of one Arnold tongue with a period-doubling curve inside a second Arnold tongue). In Ref. 11 a theory is developed that gives all possible periods of cycles at the crossing of two Arnold tongues, and the number of distinct cycles of a given period. The results continue to hold for two-dimensional extensions [e.g., Eq. (3)] if the effective dissipation is large or equivalently b is small. For numerical examples the theory holds over a finite range of b (as b increases beyond this range, the theory begins to fail for crossings with large nonlinearity), and this leads us to believe that some experiment will realize the same universal behavior. For the experimental system the crossings of Arnold tongues of low-order rationals (e.g., $\frac{1}{2}$ and $\frac{2}{3}$) occur at higher nonlinearity, and we do not expect the results of Ref. 11 to hold there (we investigated many such crossings and found that some of the cycles of Fig. 4 were absent). On the other hand, it is difficult to estimate the orbits of large periods because of experimental noise. Hence our comparisons will work best in an intermediate region, and we assume that the existence of the correct orbits is a signature that a system belongs to the universality class of Ref. 11.

We consider the crossing of an Arnold tongue T_1 of winding number $\omega_1 (=p_1/q_1)$ with a second Arnold tongue T_2 of winding number $\omega_2 (=p_2/q_2)$, where $\omega_2 > \omega_1$. For any set of parameters inside T_1 the system has two cycles of length q_1 . One of these, represented symbolically as A [for maps of form Eq. (2) the symbolic dynamics determines the cycles uniquely¹¹], has posi-

tive stability while the second, represented as \bar{A} , has negative stability. Similarly there are two cycles B (with positive stability) and C (of negative stability) of length q_2 for any set of parameters inside T_2 . The periodic orbits present on the strange attractor at the crossing of T_1 and T_2 (see Fig. 2) are all possible combinations of A, B , and C such that C is preceded by A .¹¹ Thus all available cycles can be determined by the ternary tree structure shown in Fig. 4. The result is universal for the class of maps of the form (3), when b is sufficiently small, and depends on the crossing only through A, B , and C .

The unstable periodic points are estimated from a chaotic experimental time series as follows.^{7,14} A point belongs to an M -cycle if it returns after M iterates. Similarly, an experimental point is nearly an M -cycle if it makes a close return after M time steps. Conversely (if the series is embedded in enough dimensions), a close return implies the existence of a nearby cycle; i.e., there is a periodic point of the underlying map in the neighborhood of any close return of the experimental signal. For fixed ϵ (typically 2 to 3 orders of magnitude smaller than the signal) we collect the points which return closer than ϵ after M iterates. The collection of such points bunches into distinct domains (for a series of 32000 points each bunch typically had 50-100 points). Those further from each other than $\eta \sim 2\epsilon$ are considered distinct bunches;

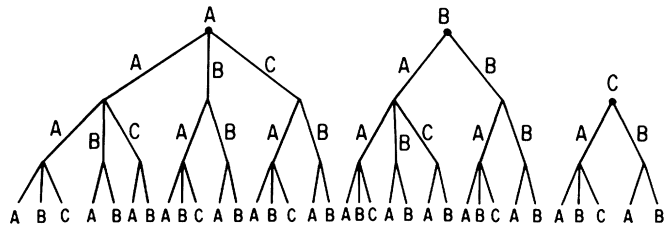


FIG. 4. The ternary tree structure which gives all orbits of a strange attractor on an annulus at the crossing of two Arnold tongues.

TABLE I. The periodic orbits lying on three strange attractors defined by crossing of Arnold tongues.

Crossing	Period (level)	No. expected	No. found
(a) $\frac{1}{4} - \frac{3}{11}$	15 (2)	30	30
	19 (3)	38	38
	26 (3)	52	52
	23 (4)	46	46
	37 (4)	74	73
(b) $\frac{2}{7} - \frac{3}{11}$	18 (2)	36	35
	25 (3)	50	51
	29 (3)	58	58
	32 (4)	64	63
	40 (4)	80	79
(c) $\frac{1}{3} - \frac{1}{4}$	7 (2)	14	14
	10 (3)	20	20
	11 (3)	22	21
	13 (4)	26	24
	15 (4)	30	30
	17 (5)	102	Many
	19 (5)	38	37

each bunch is assumed to correspond to a periodic point of period M , which is estimated as the mean of the bunch. This averaging also reduces the effective noise by a factor $\sqrt{N_b}$, where N_b is the number of points in a bunch.

We analyzed the experimental signals from several crossings of pairs of Arnold tongues, embedding the series in three dimensions. We determined the periods of all cycles, and the number of distinct cycles of a given period. In each case we extracted 4 or 5 levels of cycles of the ternary tree structure of Fig. 4, and the results are shown in Table I. For example, Table I, section (b), presents the available cycles at the crossing of the $\frac{2}{7}$ and $\frac{3}{11}$ tongues. Thus the periods of cycles A , B , and C are 7, 11, and 11, respectively. The second level of the tree contains the cycles AA , BB , AB , and AC . The first two are identical to A and B , and are not shown. Cycles AB and AC both have period 18, and are the two 18-cycles shown in Table I, section (b). Note that our algorithm found only 35 cycle points, rather than the 36 expected. We believe that this discrepancy arises because two points of an orbit lie very close to each other. From Fig. 4 we observe that the third level of the tree consists of cycles AAA , BBB , AAB , AAC , BAC , and BAB . The first two are not shown again. Cycles AAB and AAC both have period 25, and are the two 25-cycles shown in Table I, section (b). BAC and BAB have period 29, and are the two 29-cycles shown. We also find all the orbits of the fourth level of Fig. 4. In the case of the $\frac{1}{3}$ and $\frac{1}{4}$ crossing we find all orbits up to level 5. It should be emphasized that not only did we find the correct number of orbits shown in the table, but we also did not get cycles that are not in Fig. 4. This leads us to the belief that the dynamics underlying the chaotic signal from the circuit belongs to the same universality class as Eq. (3).

We can compare the experimental signal and the models only at a finite set of points in parameter space. This is because the theory is sufficiently simple only in a few cases (e.g., crossing of two Arnold tongues), and because the experimental noise limits the maximum period of cycles that can be extracted from the chaotic signal. However, the agreement of the models and experimental results at several such points suggests that the models should describe topological properties of the chaotic attractors for an entire range of parameters. We thus conclude that the underlying dynamics for the signal from the nonlinear circuit of Fig. 1 is in the same universality class as that of Eq. (3).

In conclusion, we suggest that strange attractors can be categorized into several classes which can be characterized by universal topological features (unlike the onset of chaos, which is characterized by both topological and metric features). We have identified one such class, and shown that an experimental system belongs to it. We believe that this is the first detailed characterization of universality in an experimental system beyond the onset of chaos, and that other chaotic systems can be analyzed in the same spirit.

We acknowledge fruitful discussions with James Glazier, Leo Kadanoff, and Itamar Procaccia. This work was supported in part by the Office of Naval Research through Grants No. N00014-84-K0312 and No. N00014-89-J1337.

¹M. J. Feigenbaum, J. Stat. Phys. **19**, 25 (1978).

²S. J. Shenker, Physica (Amsterdam) **5D**, 405 (1982); **5D**, 411 (1982).

³M. J. Feigenbaum, Commun. Math. Phys. **77**, 65 (1980).

⁴P. Grassberger, Phys. Lett. **97A**, 224 (1983); H. G. E. Hentschel and I. Procaccia, Physica (Amsterdam) **8D**, 435 (1983).

⁵T. Halsey, M. H. Jensen, L. P. Kadanoff, I. Procaccia, and B. I. Shraiman, Phys. Rev. A **33**, 1141 (1986).

⁶J. Glazier, G. H. Gunaratne, and A. Libchaber, Phys. Rev. A **37**, 418 (1988); M. H. Jensen, L. P. Kadanoff, A. Libchaber, I. Procaccia, and J. Stavans, Phys. Rev. Lett. **55**, 2798 (1985).

⁷A. Belmonte, M. J. Vinson, J. Glazier, G. H. Gunaratne, and B. Kenny, Phys. Rev. Lett. **61**, 539 (1988).

⁸P. Cvitanović, G. H. Gunaratne, and I. Procaccia, Phys. Rev. A **38**, 1503 (1988).

⁹P. Cvitanović, Phys. Rev. Lett. **61**, 2729 (1989).

¹⁰G. H. Gunaratne and I. Procaccia, Phys. Rev. Lett. **59**, 1377 (1987).

¹¹G. H. Gunaratne, M. H. Jensen, and I. Procaccia, Nonlinearity **1**, 157 (1988).

¹²D. G. Aronson, M. A. Chory, G. R. Hall, and R. D. McGehee, Commun. Math. Phys. **83**, 303 (1982).

¹³A. Cummings and P. S. Linsay, Phys. Rev. Lett. **60**, 2719 (1988); Physica (Amsterdam) (to be published).

¹⁴D. Auerbach, P. Cvitanović, J. P. Eckmann, G. H. Gunaratne, and I. Procaccia, Phys. Rev. Lett. **58**, 2387 (1987); M. Sano and Y. Sawada, Phys. Rev. Lett. **55**, 1082 (1986).